Geotechnical Engineering for the Preservation of Monuments and Historic Sites III – Lancellotta, Viggiani, Flora, de Silva & Mele (Eds)
© 2022 Copyright the Author(s), ISBN 978-1-003-30886-7
Open Access: www.taylorfrancis.com, CC BY-NC-ND 4.0 license

Soil contribution on the structural identification of a historical masonry bell-tower: Simplified vs advanced numerical models

A. De Angelis, A. Ambrosino & S. Sica
Department of Engineering, University of Sannio, Benevento-Italy

P.B. Lourenco
Institute for Sustainability and Innovation in Structural Engineering (ISISE), University of Minho, Portugal

ABSTRACT: In the last decade, structural identification techniques through dynamic in situ tests have been widely used to investigate the global dynamic behavior of ordinary buildings and built cultural heritage. The choice of proper boundary conditions at the base of the structure, however, is still a critical point in the development of sound numerical models able to reproduce building dynamic response reliably. The contribution of the foundation soil should be ascertained and, if necessary, properly modelled. The paper tries to shed light on the issue of soil-structure-interaction on the structural identification of masonry towers, with reference to the case study of the bell tower of Santa Sofia Church in Benevento (Italy). The experimental results of the dynamic identification, i.e. frequencies and modal shapes, have been interpreted and employed to calibrate both simplified and advanced numerical models of the soil-foundation-tower system. In the first case, soil compliance is represented by a set of springs attached at the base of the tower, which has been modelled as a 1D system. In the second case, a 3D finite element model comprehensive of the tower, the soil and the foundation structure has been developed. Pros and cons of the two numerical approaches on the structural identification process are highlighted and discussed.

1 INTRODUCTION

For historical constructions, invasive tests should be limited as much as possible. At the same time, it is of paramount importance to ascertain accurately the geometry and the mechanical properties of the construction materials together with the architectural or structural interventions carried out during the monument life. For this reason, structural identification by in-situ dynamic tests has received greater attention in the field of historical and monumental assets (Karatzetzou et al. 2015). In-situ dynamic tests turn to be useful tools to obtain the dynamic response in terms of frequencies and modal shapes (Brincker et al. 2001) and to understand different other aspects of historical building response, included the contribution of soil-structure interaction (SSI).

Among historical constructions, masonry towers may be considered as the main distinctive elements of the artistic heritage of many countries worldwide. It is widely recognized that SSI may strongly affect the dynamic behavior of slender structures like towers. Therefore, for an accurate interpretation of both frequencies and modal shapes detected on site, the role of SSI on the overall dynamic response of the building should be comprised, discerning whether the interaction itself is effective or not (De Angelis et al. 2017) and its potential impact on numerically derived modal shapes.

A proper modelling of the constraint between the tower and the soil, thus, is still a critical issue (Kouroussis et al. 2011) as different levels of complexity may be adopted. The most refined models are based on a continuum approach for both the structure and the soil. These methods are very demanding, so their use is typically restricted to handle single case studies (Casciati & Borja 2004; Cattari et al. 2019; De Silva et al. 2018).

 DOI 10.1201/9781003308867-70

In simpler models, the soil and the foundation are hidden in sets of springs and dashpots applied at the base of the structure while the structure is simulated through single or multi-degree-of-freedom systems. Springs and dashpots, encompassing soil stiffness and damping terms in the impedance function definition (Gazetas 1991), may be easily obtained through closed-form solutions available in literature. In the last decade, this type of models have been applied extensively to reproduce the experimental results from dynamic identification (Ceroni et al. 2014; Cosentini et al. 2015; Ripepe et al. 2014).

It is worth pointing out that the available solutions for quantifying soil impedance are based on many simplified assumptions on both foundation and soil features. For existing masonry structures, many unknown parameters such as the foundation embedment and geometry, or ageing effects in the construction materials may complicate the analytical impedance function computation (Piro et al. 2019). Moreover, the overburden pressure due to the structural self-weight can significantly influence the stress-dependent stiffness of the shallowest soil layers. All these aspects should be taken into account in modelling choices.

In the paper, the role of soil-structure interaction on the structural identification of a historical masonry tower is investigated by adopting both a simplified and a complete numerical method. The final goal is to quantify the impact of different numerical models accounting for SSI on the structural identification of a masonry tower.

2 THE CASE STUDY

2.1 *The structural data*

The bell tower of S. Sofia in Benevento (Italy) together with the church, the monastery and the fountain constitutes the "S. Sofia" monumental complex, which has been recognized as a UNESCO site since 2011. The tower (about 26 m high), reconstructed in 1703, has a square base and a hollow cross-section, consisting of a main body, belfry and pinnacle (Figure 1).

The side at the base is about 5.2 m, reducing to 4.8 m at the level of the belfry. An octagonal cell (about 1.5 m high) and a pyramidal cusp constitute the top of the tower. A stone stair runs along the tower from the base to the belfry and two masonry vaults, on the floor at 12.70 m and above the belfry, are present.

An accurate investigation through a photographic survey with a drone combined with direct in-situ inspections was performed to identify the elevation as well as the cross-sections of the tower. In particular, the wall thickness vary from 1.10 to 0.50 m at different levels.

Regarding the masonry texture, the tower comprises facing masonry with an external leaf, made of regular prismatic-shaped stones approximately 25 cm thick (masonry M1) and an internal leaf characterized by regular shape stones (M2) for the shaft. Conversely, the inner core is made of heterogenous masonry with red clay bricks, natural stone conglomerate and medium-sized pebbles (M3) for the belfry and the circular wall of the staircase. The vaults are made of solid brick masonry (M4).

2.2 *The geotechnical data*

The geotechnical characterization at the tower site was achieved by merging data from different sources, like the Level-1 Microzonation study of the city of Benevento (Sica & Romito 2017) or published in Senatore et al. (2019), and data obtained from the geotechnical and geophysical investigations performed *ad hoc* nearby the tower as detailed in De Angelis et al. (2022).

The soil deposit underneath the tower is made of three layers (Figure 2a), whose main physical and mechanical parameters have been summarized in Table 1. Starting from the ground level, the soil layers consist of: an Artificial filling (AF) up to a depth of about 3 m, which includes several types of waste material and reworked soil derived from excavations as well as demolition and/or restructuring of civil ancient buildings; Yellow sands (YS) between the depths of 3 m and 13 m

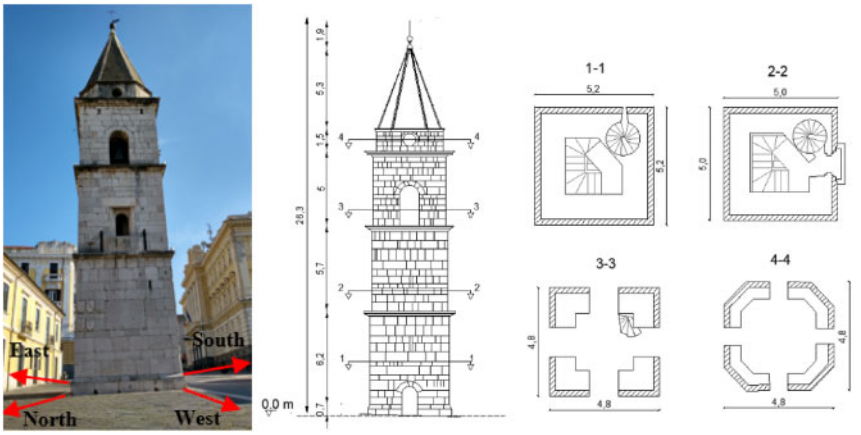

Figure 1. The bell tower of S. Sophia.

(the upper 5 meters of this layer still contain anthropic reworked deposits of the ancient city); well-cemented Conglomerate (CC) between 13 m and 47 m of depth. In Figure 2b the soil stratigraphy, which is typical of the upper part of the city of Benevento, has been combined to the shear wave velocity profile, Vs, measured on site through a MASW test (De Angelis et al., 2022). A Poisson coefficient, ν, of 0.3 was assumed for all materials.

Table 1. Soil properties.

Layer	Depth m	Vs m/s	γ kN/m^3	G MPa
AF	0–3	270	17	120
YS	3–13	640	20	820
CC	13–47	1340	23	4100

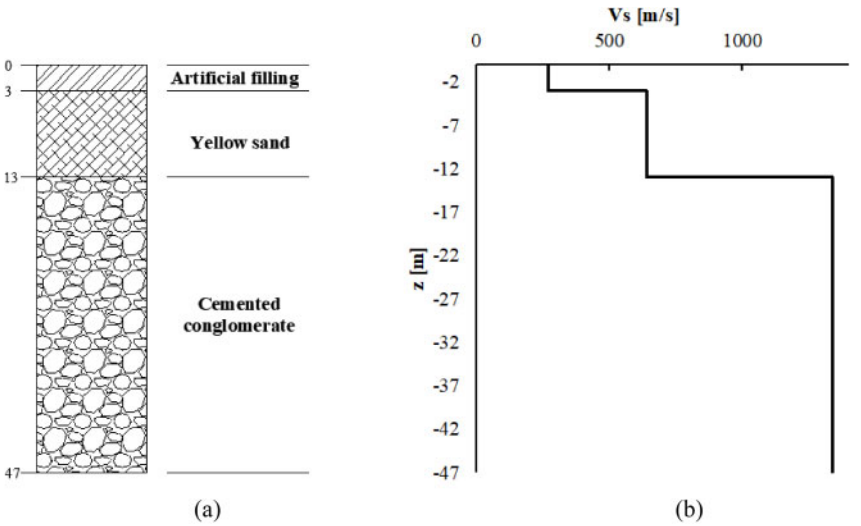

Figure 2. (a) Soil stratigraphy and (b) profile of shear wave velocity Vs.

The foundation of the tower is 2 m deep with a plan 6.5 m *x* 6.5 m, considering an enlargement of 0.50 m with respect to the base of the tower. The masonry of the foundation (M5) is assumed the same of the tower shaft; however, to consider the effect of deterioration of buried structural elements, a reduction of 15% of the Young's modulus of the foundation masonry with respect to the value attributed to the superstructure was considered.

2.3 *The ambient vibration test*

The ambient vibration test (AVT) was carried out under environmental actions (wind and human activities). The measurement chain consists of a 16-channel data acquisition system, tri-axial MEMS piezoelectric accelerometers with a nominal sensitivity of about 1 V/g and long transducer cables. The accelerometers were installed by means of special metal bases fixed directly on the walls with expansion anchors. The AVT was performed by recording time histories of acceleration of 30 minutes, at a sampling frequency of 1000 Hz, in seven points along the height of the tower. Then, the signals were treated by decimation and low-pass filtering, in order to reduce the dimension of the time series keeping the capacity to compute spectra up to approximately 50 Hz.

The extraction of the modal parameters from ambient vibration data was carried out by the software Artemis modal Pro (2019) using the Operational Modal Analysis (OMA). In particular, the Enhanced Frequency Domain Decomposition (Brincker et al. 2001) and the Stochastic Subspace Identification (Peeters & De Roeck 2001) methods were employed as described in detail in De Angelis et al. (2021).

The first five natural frequencies of the tower (Table 2) and the corresponding modal shapes were reliably identified. The first two modes are both translational and uncoupled; in particular, the first modal shape is parallel to the East-West direction with a natural frequency of 3.18 Hz, while the second one is parallel to the South-North direction with a frequency of 3.23 Hz. The third mode is torsional with a frequency of 12.03 Hz. Second order flexural modes were experimentally identified at frequencies 12.42 and 12.91 Hz for the N-S and E-W direction, respectively.

Table 2. Experimental frequencies.

Mode	Mode type	f_{exp} Hz
1	Bending E-W	3.18
2	Bending S-N	3.23
3	Torsion	12.03
4	2nd Bending S-N	12.42
5	2nd Bending E-W	12.91

3 MODELLING

3.1 *The advanced models*

Two advanced 3D models (Figure 3) were generated with the software MIDAS FEA NX considering different boundary conditions at the tower base: (a) Fixed base model (Case 1-A); (b) Compliant base model (Case 2-A) including the tower, the foundation and the underlying soil.

The structural geometry was obtained through geometrical survey and in-situ inspections of the tower, by paying attention to reproduce all the openings (doors and windows) and the floors (masonry vaults and concrete slabs). The tower was modelled using 8-node brick elements and trying to generate a quite refined mesh (typical mesh size around 0.2 m) so that a suitable approximation of the tower geometry and distribution of mass could be achieved. In addition, the masonry was modeled as a continuous homogeneous material. The external stone masonry leaf has been modelled as another layer of masonry with the same thickness estimated by in situ inspections. The properties chosen for the tower masonry are listed in Table 3 for the main material types identified.

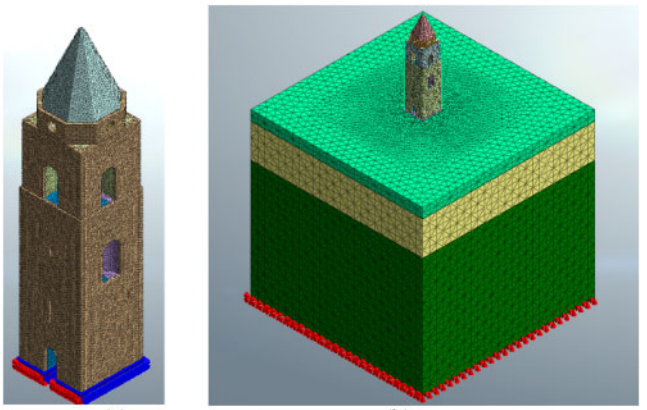

Figure 3. Advanced 3D models: (a) Fixed base and (b) Compliant-base tower.

In particular, the mechanical properties of the masonry (M1) of the external leaf were derived from literature results from double flat jacks on similar external stone layer (Bartoli et al. 2013). For the masonry (M2) of the shaft the results of a double flat-jack, performed in situ, have been adopted. Conversely, for the masonry of the belfry (M3) and vaults (M4), the maximum values of the range suggested by the Italian Code (Circolare Ministeriale n. 7, 2019) have been adopted. More details on material characterization may be found in (De Angelis et al. 2022).

The full SSI model was developed by adding to the tower the foundation structure and a suitable part of the underlying soil. The added soil volume is 47 m high with a plan of 50 m × 50 m. It was divided into three homogeneous linear elastic layers (artificial filling AF, yellow sand YS and cemented conglomerate CC), with the main physical and mechanical properties summarized in Table 1. The mesh size for the soil elements was progressively refined towards the ground surface in order to achieve a greater accuracy near the tower foundation. The nodal displacements at the base of the soil domain were fully constrained whereas boundary conditions (elastic springs) were set along the lateral sides.

Table 3. Mechanical properties of the masonries.

Element	Masonry type	E MPa	γ kN/m^3
External leaf	M1	11530	24
Shaft	M2	3730	22
Belfry	M3	1050	19
Vaults	M4	1800	18
Foundation	M5	3170	22

3.2 *The simplified models*

The simplified finite element model of the bell tower, developed with the same software MIDAS FEA NX used for the advanced analyses described in section 3.1, was obtained by discretizing the actual geometry of the tower into beam elements with a hollow-square section; the wide and thickness of the beam elements are variable along the height of the tower to match the real geometry detected by surveying and described in section 2. The mechanical properties of the masonry are reported in Table 3.

As for the advanced approach, two simplified models were also considered: 1) a fixed base beam, i.e., a cantilever scheme and 2) a beam on a flexible base made of translational and rotational springs simulating the soil-foundation interaction. To better characterize soil compliance, the deformability

of the foundation masonry and the effect of the overburden pressure induced in the subsoil by the self-weight of the tower were considered too. The stiffness of the springs were, hence, computed through well-known impedance literature formulations for embedded-rigid or embedded-flexible shallow foundations on an equivalent homogeneous soil deposit.

The following five analysis cases were solved through the simplified approaches:

- Case 1-S: Tower on fixed-base
- Case2-S: Tower on embedded Rigid foundation
- Case 3-S: Tower on embedded Flexible foundation
- Case 4-S: Tower on embedded Rigid foundation including the overburden pressure
- Case 5-S: Tower on embedded Flexible foundation including the overburden pressure

3.2.1 *Characterization of soil-foundation compliance*

The impedance functions are complex and frequency-dependent functions, which link the force (or moment) acting on an oscillating rigid foundation to the soil displacement (or rotation). They are composed of a real part, representing the dynamic stiffness of the soil-foundation system, and an imaginary part accounting for damping (radiation plus hysteric).

Classical solutions for the impedance function may be written as proposed by Luco and Westman (1971) and Veletsos and Wei (1971):

$$\overline{k_j} = k_j + i\omega c_j \tag{1}$$

where $\overline{k_j}$ denotes the complex-valued impedance function; j is an index denoting the oscillating mode (displacement or rotation) of the foundation; k_j and c_j denote the frequency-dependent soil-foundation stiffness and dashpot coefficients, respectively; ω is the circular frequency (rad/s) of the input vibration.

Pais and Kausel (1988), Gazetas (1991), and Mylonakis et al. (2006) reviewed the available impedance solutions or developed new ones with the structure of Equation 1. In particular, for a rigid rectangular foundation embedded in a half-space, Equation 2 provides for the stiffness terms, kj, of the impedance function (real part) as function of the foundation characteristic dimensions, B, soil shear modulus, G, and Poisson's ratio, ν.

$$k_j = K_j \cdot \alpha_j \cdot \eta_j \tag{2a}$$

$$K_j = GB^m f(B/L, \nu) \tag{2b}$$

$$\alpha_j = f(B/L, a_0) \tag{2c}$$

$$\eta_j = f(B/L, D/B, d_w/B, A_w/BL) \tag{2d}$$

In Equation 2, Kj is the static stiffness of the soil-foundation system at zero frequency while, α_j and η_j are the dynamic stiffness and embedment modifiers, respectively.

In the following, the equations provided by Pais and Kausel (1988) to account for the foundation embedment have been adopted.

To take into account the foundation flexibility, the spring stiffness was reduced according to the approach proposed by Pitilakis et al. (2014). The reduction factors for to the vertical (βv), horizontal (βh) and rocking (βr) modes are relate to the ratio between the Young's modulus of the foundation material, Ew, and that of the soil, Es, as shown in Equation 3:

$$\beta_v = 0.171 ln(E_w/E_s) + 0.326 \tag{3a}$$

$$\beta_h = 0.155 ln(E_w/E_s) + 0.295 \tag{3b}$$

$$\beta_r = \begin{matrix} 0.376(E_w/E_s)^{0.476} 0 < E_w/E_s \leq 3 \\ 0.492(E_w/E_s)^{0.208} 3 < E_w/E_s < 18 \end{matrix} \tag{3c}$$

For the S. Sofia tower, the impedance functions required for the simplified SSI model were calculated twice, once considering a rigid embedded foundation and another a flexible embedded

foundation. In addition, the layered subsoil (Figure 2) was modeled as a homogeneous half-space in the tower pressure bulb, by computing an equivalent shear wave velocity for each vibrating mode of the foundation, according to Stewart et al. (2003) and NIST (2012) indications.

Table 4 reports the average soil shear wave velocity $\overline{V_s}$, with the corresponding shear modulus $\overline{G_0}$ and Young modulus $\overline{E_0}$, and the equivalent soil density, ρ. The averaged values of the above soil properties were obtained on a depth range in between the foundation level, D, and a reference depth equal to $D + z_p$, Since the tower has a square base with $B = L = 6.1$ m (Table 4) and an embeddement $D = 2.5$ m, the reference depth z_p corresponds to 3.1 m for all foundation vibrating modes. In Table 4, the Young's modulus of the foundation material, Ew, characterized as explained in section 2.2, has also been reported.

Table 4. Properties of the soil and foundation.

Soil		Foundation	
$\overline{V_s}$ (m/s)	524	L (m)	6.2
$\overline{G_0}$ (MPa)	549	B (m)	6.2
$\overline{E_0}$ (MPa)	1428	D (m)	2.5
ρ(kg/m^3)	2000	Ew (MPa)	3170

As well-known, the initial shear stiffness of the shallowest soil layers may increse due to the overburden pressure caused by the weight of the superstructure (Hardin, 1978). To take into account this effect, the free-field shear wave velocity of the soil was corrected as suggested by NIST (2012) according to Equation 4:

$$V_{s,F}(z) = V_s(z) \cdot \left(\frac{\sigma'_v(z) + \Delta\sigma'_v(z)}{\sigma'_v(z)} \right)^{n/2} \tag{4}$$

where $V_{s,F}$ (z) is the overburden-corrected shear wave velocity at depth z, V_s(z) denotes the shear wave velocity measured in the free-field at depth z, n is an exponent increasing with soil plasticity index and set equal to 0.5 in light of the granular soils investigated, $\sigma'_v(z)$ is the effective stress of the soil at depth z, and $\Delta\sigma'_v(z)$ is the increment in vertical stress due to the weight of the superstructure. The overburden pressure may be computed easily by classical elastic solutions like the one proposed by Steinbrenner (1936) and shown in Figure 4a. Figure 4b reports the comparison between the free-field shear wave velocities (black line) and the the overburden-corrected shear wave velocity (red line) between the depths $D = 2.5$ m and $D + z_p = 5.6$ m. As expected, the overburden-corrected shear wave velocity is significant only at the shallowest depths.

Then, using the overburden-corrected values of shear wave velocity, the profile depth has been discretized into layers of thickness Δ_{zi} and velocity $V_{s,F}(z)_i$ to obtain an average effective velocity of 948.5 m/s from Equation 5.

$$V_{s,avg} = z_p \Big/ \sum_{i=1}^{n} \left(\Delta z_i / \left(V_{s,F}(z) \right)_i \right) \tag{5}$$

4 STRUCTURAL IDENTIFICATION WITH ADVANCED AND SIMPLIFIED MODELS

4.1 *Structural identification through the advanced models*

A modal analysis was initially developed to compute the frequencies (f_{num}) and modal shapes (φ_{num}) for the two advanced 3D f.e. models (Case 1-A and Case 2-A) in order to discriminate the importance of SSI on the correct identification of the structural behavior.

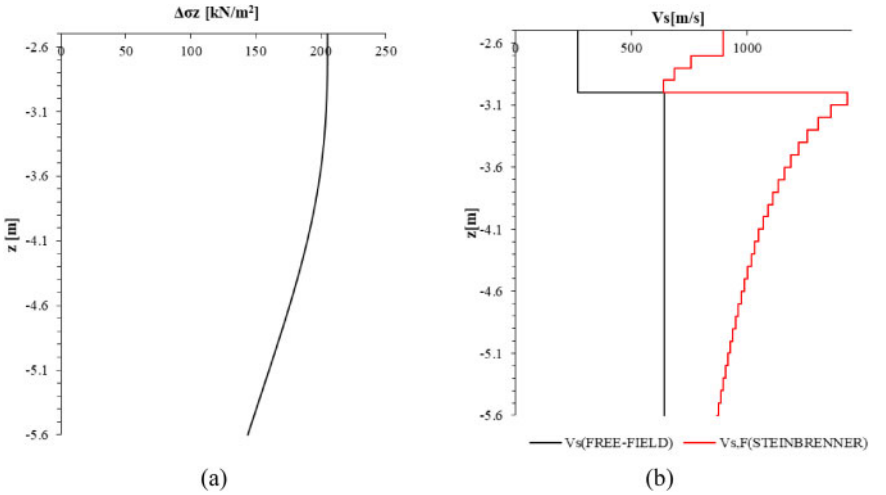

Figure 4. (a) Vertical stress increment; (b) Shear wave velocity profiles

SSI contribution on the calibration of the advanced structure model has already been detailed in De Angelis et al. (2022), by comparing the mechanical properties identified by updating the fixed-base and the compliant-base model of the bell tower. The comparison is presented in terms of frequency discrepancy, D_f, computed according to Equation 6 and modal assurance criterion MAC (Allemang & Brown 1982) in Equation 7.

$$D_f = \frac{f_{exp} - f_{num}}{f_{num}} \tag{6}$$

$$MAC = \frac{\left(\left\{\varphi_{exp}^T\right\} \cdot \left\{\varphi_{num}\right\}\right)^2}{\left(\left\{\varphi_{exp}^T\right\} \cdot \left\{\varphi_{exp}\right\}\right) \cdot \left(\left\{\varphi_{num}^T\right\} \cdot \left\{\varphi_{num}\right\}\right)} \tag{7}$$

Table 5 reports the final results of the performed model updating (De Angelis et al. 2022) that, as it could be observed, returned different optimal values for the fixed-base or the compliant-base model. The change in percentage with respect to the initial values of masonry stiffness and weight is shown in the brackets. In the case of fixed model, the two parameters affecting most the calibration of the model are the Young modulus of the external masonry stone leaf (M1) and of the masonry of the belfry (M3). A corresponding decrease of 38% and 28% with respect to the initial values adopted in the fixed model was obtained. Conversely, the influence of the specific weight of the masonries was found to be negligible (about 4%). Model updating applied to the advanced model corroborates the negligible effect of the specific weight of the masonry, which remains almost equal to the initial value adopted (5%). The final value of the elastic modulus for all types of masonry, instead, is different from the initial one of the order of 50%–110%, while it remains almost unchanged for the masonry stone leaf (M1). The comparison in terms of numerical frequencies and MACs of the updated models and the experimental results is presented in Table 6.

For the fixed model, the updating process improved the correlation of the first and the second bending modes being D_f less than 3% (4% on average). A higher value of frequency discrepancy equal to 13% was found for the torsional mode. In terms of modal shape (MAC values) the correlation may be considered globally satisfactory (minimum of 0.7 and average of 0.8), with larger errors found for the higher modes. This could be related to soil structure contribution. Actually, referring to the final correlation for the compliant model, it is possible to observe an excellent match since the average D_f is less than 4% and the maximum difference in frequencies is

Table 5. Optimal values of the masonry properties after model updating.

		Fixed model (Case1-A)		Compliant model (Case2-A)	
Element	Masonry type	E [MPa]	γ [kN/m^3]	E [MPa]	γ [kN/m^3]
External leaf	M1	7190 **(−38%)**	23.0 **(−4%)**	12146 **(5%)**	22.86 **(−5%)**
Shaft	M2	3590 **(−4%)**	21.1 **(−4%)**	6073 **(63%)**	20.95 **(−5%)**
Belfry	M3	1340 **(28%)**	18.2 **(−4%)**	2267 **(116%)**	18.10 **(−5%)**
Vaults	M4	1720 **(−4%)**	17.3 **(−4%)**	2915 **(62%)**	17.14 **(−5%)**
Foundation	M5		–	4763 **(50%)**	19 **(−14%)**

Table 6. Comparison between numerical and experimental modes.

		Fixed model (Case1-A)			Compliant model (Case2-A)		
Mode	f_{exp} [Hz]	f_{num} [Hz]	D_f [%]	MAC [%]	f_{num} [Hz]	D_f [%]	MAC [%]
1st bending E-W	3.18	3.17	−0.25	89	3.04	−4.40	92
1st bending N-S	3.23	3.31	2.57	89	3.11	−3.86	92
Torsional	12.03	10.35	−13.98	78	12.03	−0.01	82
2nd bending E-W	12.42	12.20	−1.77	76	13.28	6.92	95
2nd bending N-S	12.91	12.68	−1.78	71	13.62	5.48	91
Average (abs. value)			4.07	81	–	4.13	90

lower than 5%. Accounting for SSI, the MAC values improved significantly with excellent results (average of 0.91 and minimum value of 0.82) for the higher modes.

Therefore, the outcomes of the study underline that a good correlation with the modal shapes may be obtained only with the SSI contribution.

4.2 *Structural identification with the simplified models*

As the simplified models concern, a modal analysis was initially carried out to obtain the main frequencies, modal shapes and modal participating mass ratio in the fixed-base condition (Case 1-S). The simplified model is able to reproduce the first and second flexural modes in x and y direction, respectively. Conversely, it is not able to reproduce the torsional mode due the oversimplification of the static scheme. In Table 7, the results obtained from the simplified and the advanced models are both compared to the experimental ones. In both cases, the numerical frequencies are higher than the experimental ones. In addition, it is worth noting that with the simplified model the modes are purely flexural in a specific direction; therefore, it is not able to identify the coupling of the modes in the two directions as detected experimentally. However, the first modes in both x and y directions are the principal ones, as testified by the highest value of the participating mass, being about 60%.

If the compliant-base models are considered, the outcomes of the simplified numerical study in terms of natural frequencies and frequency mismatch with respect to the experimental values, are detailed in Table 8. Here, the different predictions corresponding to the compliant model refer to the five modes of computing the stiffness terms of the impedance function as described in section 3.2, i.e. with or without accounting for foundation masonry deformability and the effect of soil overburden pressure due to the tower weight.

As expected, the compliant base models always provide for natural frequencies lower than those of the fixed-base model. Introducing the deformability of the foundation structure (Case3-S), the

Table 7. Comparison between experimental data and numerical frequencies for the fixedbase models, both simplified (Case 1-S) and advanced (Case 1-A)

		Numerical							
Experimental		Fixed model (Case1-S)				Fixed model (Case1-A)			
Mode	f_{exp} [Hz]	Mode	f_{num} [Hz]	m_x [%]	m_y [%]	Mode	f_{num} [Hz]	m_x [%]	m_y [%]
1st bend. E-W	3.18	1st bend. x	3.76	66	0	1st bend. E-W	3.54	19	40
1st bend. N-S	3.23	1st bend. y	3.90	0	60	1st bend.N-S	3.66	40	20
Torsional	12.03	NA	–			Torsional	11.48	0	0
2nd bend. E-W	12.42	2nd bend. x	12.14	23	0	2nd bend. E-W	13.49	22	1
2nd bend. N-S	12.91	1st bend. y	15.61	0	22	2nd bend.N-S	14.02	1	20

Table 8. Comparison between experimental and numerical data for the compliant base condition.

		Numerical									
Experimental		Fixed model (Case1-S)		Compliant model (Case 2-S)		Compliant model (Case 3-S)		Compliant model (Case 4-S)		Compliant model (Case 5-S)	
Mode	f_{exp} [Hz]	f_{num} [Hz]	D_f [%]	f_{num} [Hz]	D_f [%]	f_{num} [Hz]	D_f [%]	f_{num} [Hz]	D_f [%]	f_{num} [Hz]	D_f [%]
1st bend. E-W	3.18	3.76	−18.28	3.40	−7.05	3.17	0.47	3.64	−14.50	3.40	−7.06
1st bend. N-S	3.23	3.90	−20.67	3.51	−8.68	3.25	−0.73	3.77	−16.62	3.51	−8.70
2nd bend. E-W	12.42	12.14	2.29	11.75	5.43	11.31	8.92	12.01	3.32	11.65	6.18
2nd bend. N-S	12.91	15.61	−20.88	14.53	−12.54	13.56	−5.02	15.24	−18.01	14.35	−11.14

frequencies become even lower and the mismatch between the experimental and compliant-base model reduces.

Conversely, when the overburden pressure generated in the soil by the structural weight (Case 4-S) of the tower is introduced, an overall stiffening of the system is obtained with the consequent increase of the frequencies, thus leading to a higher mismatch.

To refine the tuning process, it was decided to use the fixed base model (Case 1-S) and the most comprehensive simplified model (Case 5-S) that includes both the overburden pressure due to the structural weight and the flexibility of the foundation structure, for further updating of the structural model. The aim is to numerically reproduce the experimental frequencies and understand how such calibration changes the properties assigned to the materials of the superstructure.

The final values of the superstructure masonry stiffness are reported in Table 9. Different observation may be drawn. First, in the simplified model, the two parameters affecting most the calibration of the model in the fixed base configuration are the Young moduli of the external masonry stone leaf (M1) and of the masonry of the shaft (M2). They are characterized by a decrease of 40% and 17%, respectively. In the compliant model (Case 5-S), the final value of the elastic modulus for all types of masonry is different from the initial value in the range 9-67%. Instead, the influence of the specific weight of the masonries is negligible for both the fixed base and compliant model.

Finally, the comparison among the numerical frequencies of the updated simplified models and the experimental one is presented in Table 10. It could be concluded that an acceptable correlation

can be obtained also with the simplified model including the SSI, even though it is not able to detect the torsional mode.

Table 9. Final values of the masonry properties after a further updating of the simplified models.

		Fixed model (Case1-S)		Compliant model (Case5-S)	
Element	Masonry type	E [MPa]	γ [kN/m^3]	E [MPa]	γ [kN/m^3]
External leaf	M1	6890 **(−40%)**	23.0 **(−4%)**	8280 **(−39%)**	23 **(−4%)**
Shaft	M2	3090 **(−17%)**	21.1 **(−4%)**	4130 **(9%)**	21.5 **(−2%)**
Belfry	M3	1340 **(−4%)**	18.2 **(−4%)**	3190 **(67%)**	18.2 **(−4%)**
Foundation	M5	–	–	2650 **(−20%)**	22 **(0%)**

Table 10. Correlation between numerical and experimental modes (simplified models).

		Fixed model (Case1-S)		Compliant model (Case5-S)	
Mode	f_{exp}[Hz]	f_{num} [Hz]	D_f[%]	f_{num} [Hz]	D_f[%]
1st bending E-W	3.18	3.18	−0.08	3.25	−2.29
1st bending N-S	3.23	3.30	−2.03	3.35	−3.84
Torsional	12.03	–	–		
2ndbending E-W	12.42	10.36	16.59	11.25	9.44
2nd bending N-S	12.91	13.38	−3.62	13.96	−8.14
Average (abs. value)			5.58		5.93

5 CONCLUSIONS

The dynamic behavior of the S. Sofia bell tower in Benevento (Italy) was numerically simulated through simplified and advanced numerical models

The comparison between the experimental data obtained from an ambient vibration test, and the numerical results described in the present study evidenced that:

1) the third experimental mode which is a torsional one, cannot be reproduced by the simplified numerical models;
2) with both the simplified and advanced numerical models with restrained base, the tower frequencies are higher than the experimental ones; in addition, with the simplified model the modes are purely flexural in a specific direction and it is not able to identify the coupling of the modes in the two directions as detected experimentally;
3) by implementing the compliant base models, the natural frequencies of the coupled system decrease as expected;
4) by introducing also the foundation deformability in the simplified SSI models (Case3-S), the numerical frequencies decrease more and more and the mismatch between the experimental and compliant-base model frequencies are reduced compared to the fixed base model.
5) the simplified model of the bell tower may provide an acceptable correlation only if it includes the SSI contribution by means of base springs that accounts for the overburden pressure of the tower and the foundation masonry deformability.

ACKNOWLEDGEMENTS

The authors thank Prof. Maria Rosaria Pecce for her precious support and suggestions. This research activity was carried out within the framework of the PON Research and Innovation 2014–2020, Axis I-Investments in Human Capital, MIUR notice AIM-"International Attraction and Mobility"-Line 1, Project: AIM 1823125-3 – Cultural Heritage. Part of the work has been developed in the framework of the 2019-2021 Reluis-DPC research program funded by the Italian Civil Protection Department, as a contribution to the geotechnical Work Package Soil-Foundation-Structure Interaction (Task 16.3).

REFERENCES

Allemang, R.J., Brown, D.L. 1982. A correlation coefficient for modal vector analysis. Proceedings of the 1st International Modal Analysis Conference. Orlando, USA.

ARTeMIS Modal Pro 6.1 software. 2019. Issued by Structural Vibration Solutions ApS. NOVI Science Park, Niels Jernes Vej 10, DK 9220 Aalborg East, Denmark.

Bartoli G, Betti M, Giordano S. In situ static and dynamic investigations on the "Torre Grossa" masonry tower. Eng Struct 2013; 52:718–733

B.O. Hardin. 1978. The nature of stress-strain behavior for soils. Geotechnical Engineering Division Specialty Conference on Earthquake Engineering and Soil Dynamics, ASCE, Pasadena (California).

Brincker, R., Zhang, L., Andersen, P. 2001.Modal identification of output-only systems using frequency domain decomposition. Smart Materials and Structures; 10:441–5.

Casciati, S. & Borja, RI. 2004. Dynamic FE analysis of South Memnon colossus including 3D soil-foundation structure interaction. Comput Struct; 82:1719–1736.

Cattari, S., Sivori, D., Brunelli, A., Sica, S., Piro, A., de Silva, F. et al. 2019. Soil-structure interaction effects on the dynamic behaviour of a masonry school damaged by the 2016-2017 Central Italy earthquake sequence. Proceedings of the 7th lnternational Conference on Earthquake Geotechnical Engineering (VII ICEGE) 2019. June 17-20, Rome, Italy.

Ceroni, F., Sica, S., Pecce, M., Garofano, A. 2014. Evaluation of the natural vibration frequencies of a historical masonry building accounting for SSI. Soil Dyn Earthq Eng; 64:95–101.

Circ.2019-Instructions for "Technical Norms for Constructions".

Cosentini, R., Foti, S., Lancellotta, R., Sabia, D. 2015. Dynamic behavior of shallow founded historic towers: validation of simplified approaches for seismic analyses. Int J Geotech Eng:13–29.

De Angelis, A., Lourenço, P.B., Sica, S., Pecce, M.R. 2022. Influence of the ground on the structural identification of a bell-tower by ambient vibration testing, Soil Dynamics and Earthquake Engineering. In press, https://doi.org/10.1016/j.soildyn.2021.107102

De Angelis, A., Mucciacciaro, M., Pecce, M.R., Sica, S. 2017. Influence of SSI on the Stiffness of Bridge Systems Founded on Caissons. J. Bridge Eng., 22(8): 04017045.

De Angelis, A., Santamato, F., Pecce, M.R. 2021. Assessment of an historical masonry bell tower by modal testing. The 8th workshop on Civil Structural Health Monitoring CSHM-8. March 29–31, 2021.

De Silva, F., Pitilakis, D., Ceroni, F., Sica, S., Silvestri, F. 2018. Experimental and numerical dynamic identification of Carmine bell tower in Naples (Italy). Soil Dyn Earthq Eng; 109:235–250.

Gazetas, G. 1991. Foundation vibrations," Foundation Engineering Handbook, 2nd Edition, Chapter 15, H.-Y. Fang, ed., Chapman and Hall, New York, New York.

Karatzetzou, A., Negulescu, C., Manakou, M., Francois, B., Seyedi, D., Pitilakis, D., Pitilakis, K. 2015. Ambient vibration measurements on monuments in the Medieval City of Rhodes, Greece. Bull. Earth.Eng;13(1):331–345.

Kouroussis, G., Verlinden, O., Conti, C. 2011. Finite dynamic model for infinite media: the corrected solution of viscous boundary efficiency. J Eng Mech; 137 (7):509–511.

Luco, J.E., and Westmann, R.A.1971. Dynamic response of circular footings, Journal of Engineering Mechanics, Vol. 97, No. 5, pp. 1381–1395.

Midas FEA NX- Midas Engineering Software–Manual

Mylonakis, G., Nikolaou, S., and Gazetas, G. 2006. Footings under seismic loading: Analysis and design issues with emphasis on bridge foundations. Soil Dynamics and Earthquake Engineering, Vol. 26, pp. 824–853.

NIST. 2012. Soil-structure interaction for building structures. Technical report, US Department of Commerce, Washington, DC.

Pais, A., and Kausel, E. 1988. Approximate formulas for dynamic stiffnesses of rigid foundations. Soil Dynamics and Earthquake Engineering, Vol. 7, No. 4, pp. 213–227.
Peeters, B., De Roeck, G. 2001. Stochastic System Identification for Operational Modal Analysis: A Review. Journal of Dynamic Systems Measurement & Control;123(4):659–67.
Piro, A., de Silva, F., Parisi, F., Scotto di Santolo, A., Silvestri, F. 2019. Effects of soil-foundation-structure interaction on fundamental frequency and radiation damping ratio of historical masonry building sub-structures. Bullettin Earthq Eng;18: 1187–212.
Pitilakis D, Karatzetzou A. 2014. Dynamic stiffness of monumental flexible masonry foundations. Bullettin Earthq Eng;13:67–82.
Ripepe, M., Coli, M., Lacanna, G., Marchetti, E., Cristofaro, M., De Stefano, M., Mariani, V. et al. 2014. Dynamic response of the Giotto's bell-tower, in: Proceedings Engineering Geology for Society and Territory – Turin 15–19, 2014; Vol. 8- Preservation of Cultural Heritage, pp. 323–27.
Senatore, M.R., Boscaino, M., Pinto, F. 2019. The Quaternary geology of the Benevento urban area (southern Italy) for seismic microzonation purposes. Ital. J. Geosci.; Vol. 138, pp. 66–87.
Sica, S., Romito, M. 2017. Convezione tra il Dipartimento di Ingegneria e il Comune di Benevento nell'ambito della Manifestazione di interesse per la realizzazione di indagini e studi di Microzonazione sismica ai sensi dell'OPCM 3907 del 13-11-2010; (in Italian)
Steinbrenner, W. 1936. A rational method for determination of the vertical normal stresses under foundations, Proceedings of the International Conference on Soil Mechanics and Foundation Engineering, Cambridge, Massuchusetts, 142–143.
Stewart, J.P., Kim, S., Bielak, J., Dobry, R., and Power, M. 2003. Revisions to soil structure interaction procedures in NEHRP design provisions," Earthquake Spectra, Vol. 19, No. 3, pp. 677–696.
Veletsos, A.S., and Wei, Y.T. 1971.Lateral and rocking vibrations of footings,"Journal of Soil Mechanics and Foundations Division, Vol. 97, No. 9, pp. 1227–1248.